Engineering and Technology Journal

The Fundamental of Reduced Graphene Oxide with Nanosilver Composite Films Using the Spin Coating Technique

Hamsa A. Alaloosi [a] *, **Farah T. M. Noori [b]**, **Abdulhadi K. Jidran** [ID] [c]

[a, c]Laser and Optoelectronics Engineering Dept, University of Technology-Iraq, Alsina'a street, 10066 Baghdad, Iraq.

[b]Physics Dept, Baghdad University-Iraq, Baghdad, Iraq

*Corresponding author Email: ha660569@gmail.com

HIGHLIGHTS

- The preparation films have good properties in electronic devices, with an energy gap decreasing from 3.4 to 3.1ev with the increase of AgNPs.
- The extinction coefficient has the maximum value in the visible region.
- The absorption coefficient shows the highest value at 300nm for rGO: AgNPs, and it
- The increase of silver nanoparticle concentration increases the extinction coefficient values, similar to absorption coefficient behavior.

ABSTRACT

Graphene oxide synthesis by hummers method and reduction by the green chemical method using green tea. Preparation films with reduced graphene oxide (rGO) and Silver Nanoparticles (AgNPs) by a spin coating method. The preparation films and Nanomaterial characteristics with X-Ray diffraction (XRD) GO has a peak at ($2\theta = 11.22°$). While rGO has a wider peak at ($2\theta = 26.2°$). The (rGO +AgNPs) films have five obvious diffraction angles. In Scanning electron microscopy (SEM) and energy-dispersive X-ray spectroscopy (EDX), flaky sheet (rGO), and spherical (AgNPs) with Nanosize about ~20 nm, the peaks of EDX indicated the presence of Carbon, silver, and oxygen. The energy gap was calculated from the absorbance spectrum and seemed to decrease with increasing AgNPs.

ARTICLE INFO

1. Introduction

Recently, scientists studied graphene oxide (GO) and reduced graphene oxide (rGO) to exhibit their application in different fields [1]. Huge challenge to produce (rGO) because of using hazardous chemicals such as hydrazine hydrate; therefore, the researchers used several green reducing agents as an alternative method to produce (rGO) [2]. So it used green tea leaves as a reduction agent (green synthesis method) [3]. The development of Nano-materials, including inorganic materials such as silver Nanoparticles and AgNPs, has several excellent physical, chemical, and biological properties that have been reported for AgNPs [4,5]. The rGO- AgNPs Nanocomposites were prepared by a spin coating method. This Nanostructure rGO- AgNPs are used together to enhance their properties, such electrical, optical, thermal conductivity, higher antimicrobial, and catalytic activities. These Nanocomposites have been developed in different applications (detector, electronics, electrochemical bio-sensing, and catalysis) [6-9]. This study uses graphene oxide synthesis by hummer's method, while rGO synthesis uses green tea leaves. Finally, rGO- AgNPs Nanocomposite films preparation by a spin coating method. The film's characterization by XRD, SEM, EDX, FTIR, and UV – Vis, respectively.

2. Experimental Wor

2.1 Material

The materials used are Graphite rod 99.995%, $KMnO_2$, 99%, $NaNO_3$,99.5%, H_2O_2,32% and HCl,37.5% from (Sigma-Aldrich) and (H_2SO_4,98%) from (LOBA Chemie) and green tea leaves, Poly Methyl Methacrylate (MERCK), toluene (Sigma-Aldrich), and silver Nanoparticles (Sigma-Aldrich).

2.2 Synthesis of (GO) and rGO

The fundamental material used by Hummer for the synthesis of graphene oxide is the processing of powder from the graphite rods. In that synthesis, 1 g of graphite powder and 0.5 g of $NaNO_3$ were applied (in an ice bath container) to the sulfuric acid. This was followed by the slow addition of 3 g of $KMnO_2$ at a temperature of around 40℃. Besides, a magnetic stirrer is used at 30℃ for 30 hours for mixing. By inserting 5 ml of 32 percent H_2O_2, the reduction of $KMnO_2$ is carried out. This forms the color of the mixture to light brown and finally washes the mixture with deionized water and 5% HCl (HCl (11.52) + H_2O (88.75)) ml. Finally, to achieve solid graphene oxide, the substance was dehydrated at 70℃ for 5h. (rGO) synthesis by a green chemical process which was Formulated by adding (0.09375 g) of graphene oxide in (75 ml) of green tea. The filter paper was used to filter the green tea solution. The mixture was placed on an ultrasonic for 1 hour and then on a magnetic stirrer for 2.5 hours at a temperature of less than 90℃. The product was filtered and dried in an oven for 3 hours at a temperature below (80℃).

2.3 Sample Preparation by Spin Coating

The liquid samples of (r GO +Ag) with different proportion (r GO (0.15 g/25ml) +Ag ((0.015, 0.025, 0.035)) will deposition on (glass + Si – p-type) slides. with the high-speed rotation of the substrate (typically >10 rotations per second = 600 rpm). The surface of a spinning substrate is coated (cast) with a solution of the desired material in a solvent. A liquid solution is deposited onto a rotating substrate to form a thin layer of solid material. The deposited substrate will be annealing at 70˚C for 2h and be characterized by XRD, SEM, EDX, FTIR, and UV-Vis.

3. Results and discussion

3.1 X-Ray Diffraction XRD

The XRD model (X-Ray Shimadzu 6000) spectra of GO and rGO are given in figure1a. GO contains a peak at ($2\theta = 11.22°$) with d- spacing (7.87 Å). This peak indicates the successful production of graphene oxide by this method. Because of the oxygen functional group formed, the d – spacing of graphite increased (d = 4.35 A) because of carboxyl, hydroxyl, and epoxy that lay between the graphite. [10, 11]. rGO exhibits a wider peak at ($2\theta= 26.2°$) with d- spacing (4.87 A), which improves the removal of the functional oxygen group. GO, and rGO both have a hexagonal structure. [12, 13]. While, figure1 b illustrate the XRD spectra of AgNPs with peaks at ($2\theta = 38.1829°$, $44.3727°$, $64.53°$) with plan ((111), (200), (220)) respectively [14]. (r GO +AgNPs) films illustrated in figure1 c The five obvious diffraction peaks ($2\theta = 27.77°$, $32.32°$, $46.22°$, $67.27°$, $75.87°$) with the plan ((100), (111), (200), (220) (311)) respectively planes of face-centered cubic (FCC) crystalline structure, respectively, suggesting that AgNPs exist in the crystalline state [14]. Used Debye-Scherrer's Equation to determine the average crystallite size:

$$D = \frac{K\lambda}{\beta cos\theta} \tag{1}$$

Where D is the crystallite size, λ is x-ray wavelength (1.54178 A°), β is full width at half maximum (FWHM) of the observed peak, and θ is the diffraction angle. By resolving the greatest intensity peak, the average crystallite size was estimated. The average crystallite size was calculated. (D_{ave}= 8.95 nm, 7.67 nm, 22.719 nm, 71.25 nm) for (GO, rGO, AgNPs and rGO+ AgNPs) respectively.

3.2 Scanning Electron Microscopy (SEM) and Energy Dispersive X-ray Spectroscopy (EDX)

SEM type (MIRA3FEG-SEM) images shown in Figure 2. a, b, and c (rGO + Ag) films, it was found AgNPs are deposited and prevail on Nano reduced graphene flakes, the average particles size of AgNPs is about ~25 nm. Because of the strong electrostatic and electrical contact between rGO flakes and AgNPs, AgNPs were deposited on them. [15].Using energy-dispersive X-ray spectroscopy (EDX), elemental compositional analysis of (rGO + Ag) Nano-composite films was determined. The C, O, and Ag signals verified the direct-mapped (rGO + Ag) Nano-composite films [16].

3.3 Fourier Transmission Infrared (FTIR)

Figure 3 displays the FTIR model (SHIMADZU) spectrum for GO and rGO. This test was carried out to determine the functional groups of oxygen contained in the materials. In addition, reduced graphene oxide is projected to have less oxygen than graphene oxide. Figure 3a shows GO spectra, a sharp board peak located at 3421 cm–1, indicating the presence of the O-H hydroxyl group and the peak C=O stretching at 1681 cm-1. Also, the epoxy group C-O-C and C-O stretch at 1222 cm-1 and 1063 cm-1, respectively [2]. Oxygen group presence indicated the successful synthesis of graphene oxide [17]. For rGO spectra in Figure 3, the peak 3421 cm^{-1} disappears [18]. The new peak C=C was Noticed at 1737 cm-1 [19]. The peak at 1681 cm^{-1} is less intense than GO because of the oxygen removed by the green tea leaves [20]. In the case of (rGO + AgNPs) films

(S(A, B, C) figure 3 b, The strength of the peaks owing to carbonyl and other groups decreases further as a result of the development of AgNPs on the surface of rGO[21].

3.4 Ultraviolet-Visible Light Spectroscopy (UV-Vis)

In UV- Vis type (UV-1280 and UV1900 Shimadzu) spectrum of (rGO + Ag) films, absorbance peak illustrate in figure3(a), a sharp peak appears at 245 nm for rGO + Ag which due to the presence of rGO and e to the $\pi \rightarrow \pi*$ transitions of aromatic C-C bonds. While in film rGO + Ag3 peak appears at 422 nm, these peaks' appearances are compatible with the development of silver nanoparticles on the flaks surface, which correlates to the typical surface (Plasmon resonation) [22, 23]. The bandgap of the rGO + Ag Nano-composite was calculated using Tauc equation [22]:

$$\alpha h\nu = D(h\nu - E_g)^n \tag{2}$$

Here, α is the absorption coefficient, hv is the incident photon's energy, Eg is the optical band gap energy, D is a constant and n is an index and can have values i.e. 2, 3, 1/2 1/3, which depends on the band to band transitions. The transition data enables the best linear fit in the band edge region for n = 1/2. The plot of $(\alpha h\nu)$ 2 vs. hv is shown in Figure 3(b, c, d). The energy gap decreases with increasing the Ag nanoparticles from 3.4 eV to 3.1 eV [24, 25].
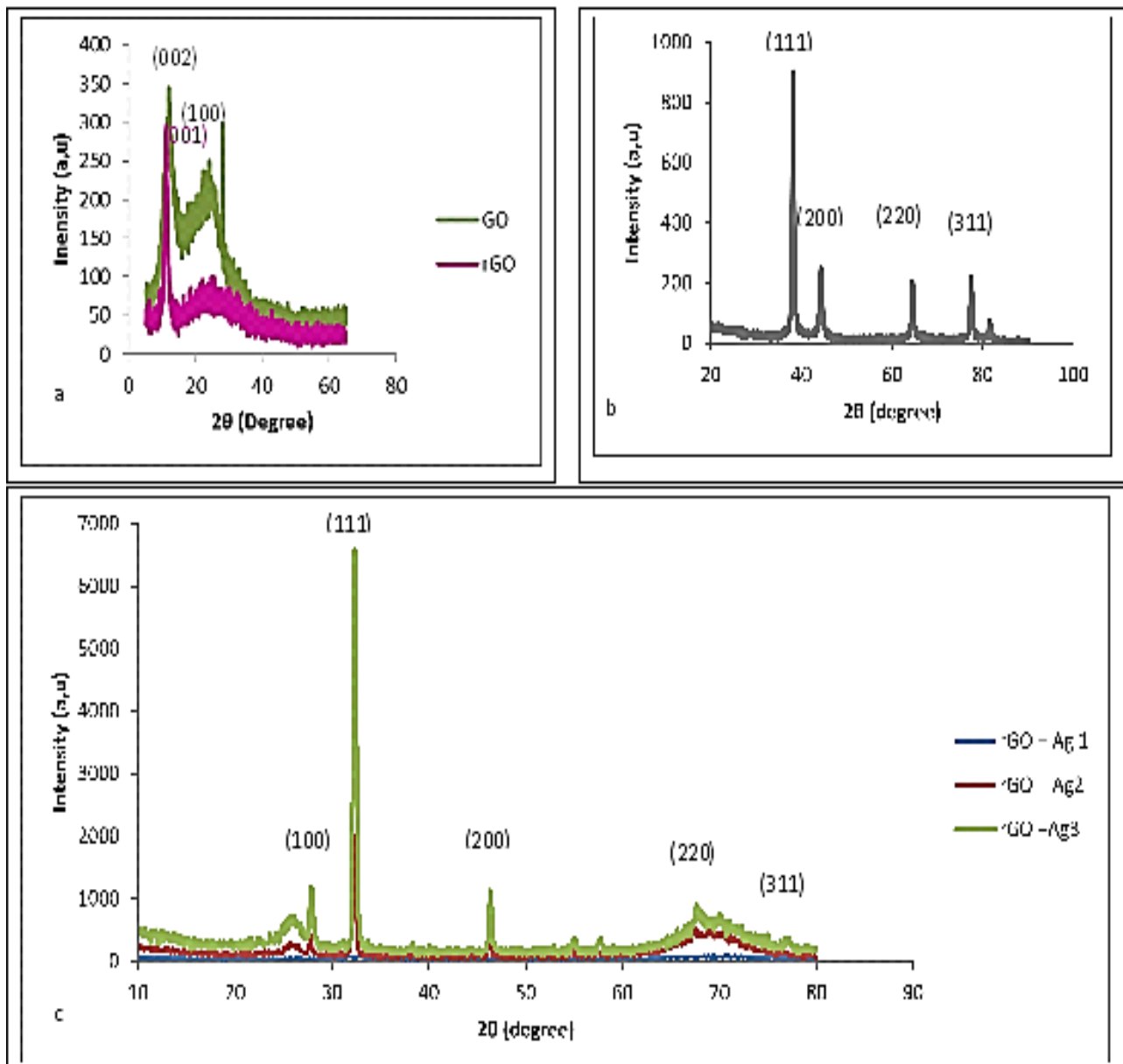

Figure 1: Illustrate the XRD spectrum of (rGO: AgNPs 1, 2, and 3) thin films prepared by Spin Coating model (SPC-TN-556).
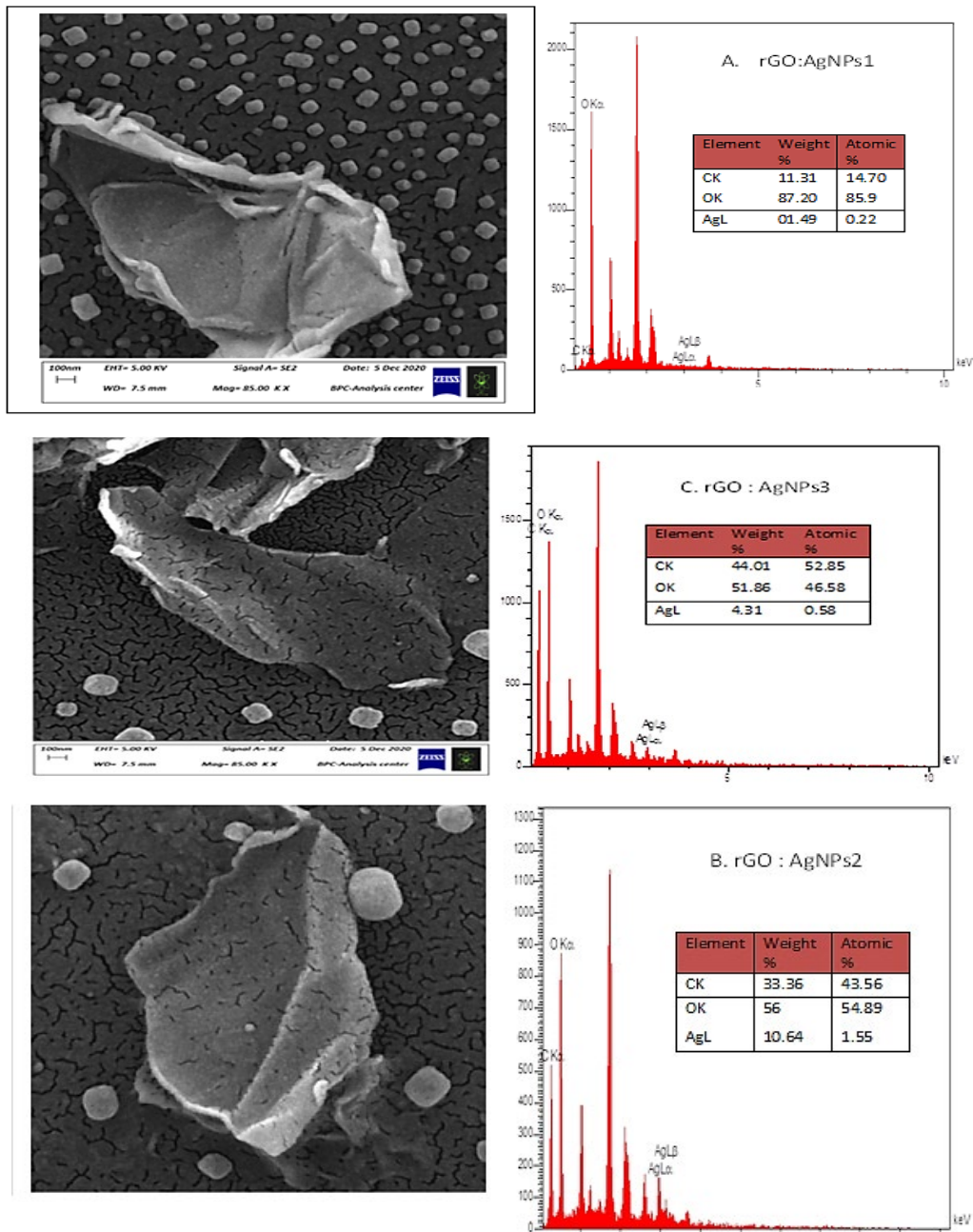
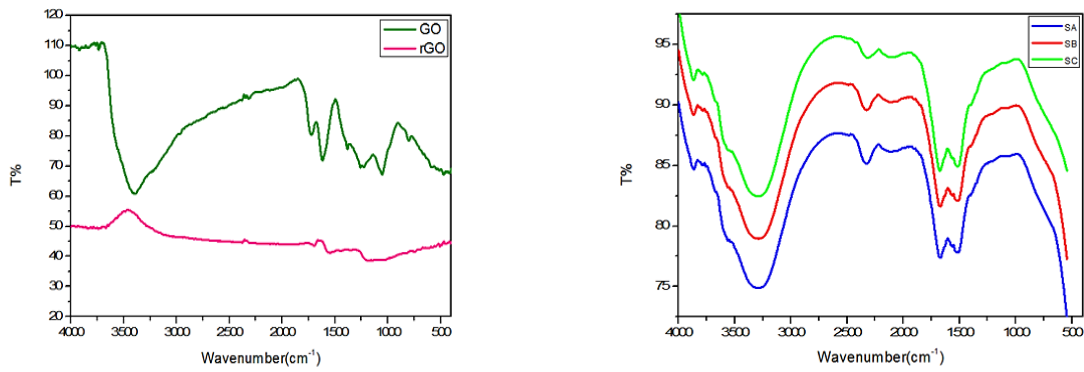**Figure 2:** a, b, and c show SEM and EDX images of (rGO + Ag) films

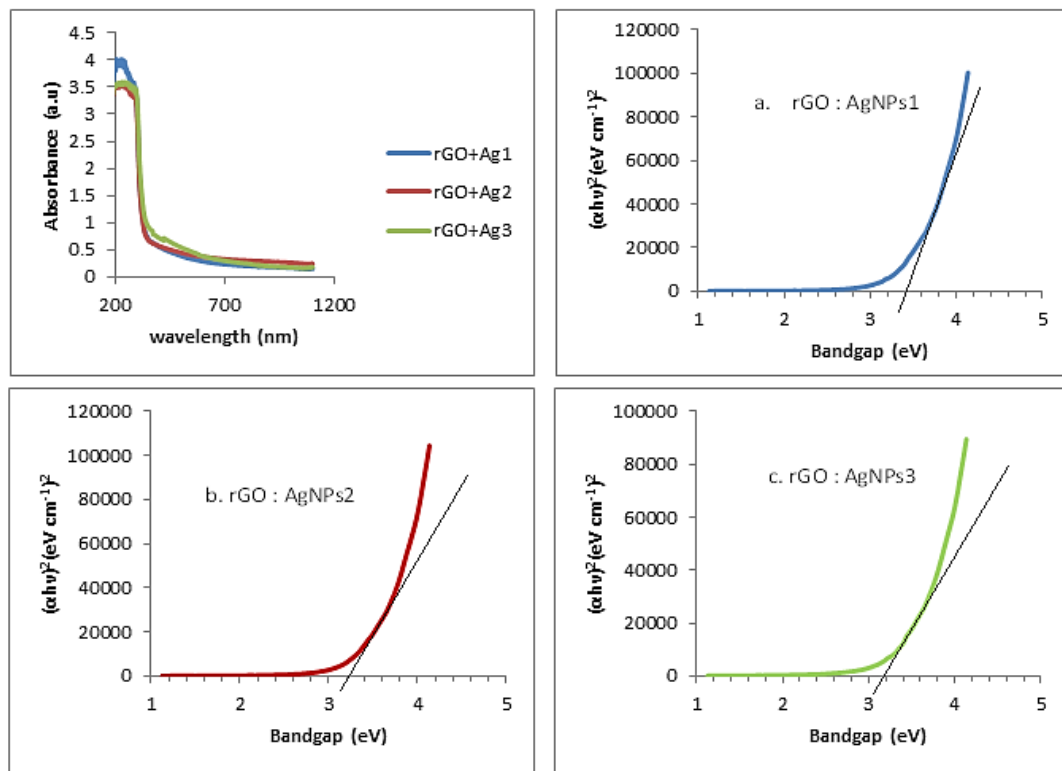**Figure 3:** Demonstrates FTIR spectrum for a. GO and rGO. and b. rGO + AgNPs films by spin coating

Figure 4: a. absorbance of GO and rGO b, c, d, Bandgap of rGO + AgNPs films.

4. Conclusion

Flakey sheet of reduced graphene oxide in Nanoscale and spherical silver Nanoparticles illustrated in the scanning electron microscopy (SEM). The preparation films have good properties in electronic devices with an energy gap decreasing from 3.4 to 3.1ev with increasing AgNPs. The extinction coefficient has a maximum value in the visible region. The increasing silver nanoparticle concentration increases the extinction coefficient values, similar to absorption coefficient behavior. While the absorption coefficient shows the highest value at 300nm for rGO:AgNPs, and it decreases until it vanishes at a wavelength of 1100nm.

Author contribution

All authors contributed equally to this work.
Data availability statement

The data that support the findings of this study are available on request from the corresponding author.
Conflicts of interest

The authors declare that there is no conflict of interest.

References

[1] W. Lv, D.-M. Tang, Low-Temperature Exfoliated Graphenes: Vacuum-Promoted Exfoliation and Electrochemical Energy Storage, ACS Nano, 3 (2009) 3730–3736. https://doi.org/10.1021/nn900933u

[2] Y. Hernandez, V. Nicolosi, High-yield production of graphene by liquid-phase exfoliation of graphite, Nat. Nanotechnol., 3 (2008) 563–568. https://doi:10.1038/nnano.2018.215

[3] J. Zhang, H. Yang, G. Shen, P. Cheng, J. Zhang, S. Guo, Reduction of graphene oxide vial - ascorbic acid, Chem. Commun., 46 (2010) 1112–1114 . https://doi.org/10.1039/B917705A

[4] M. A. Faramarzi, A. Sadighi, Insights into biogenic and chemical production of inorganic nanomaterials and nanostructures, Adv. Colloid Interface Sci., 189−190 (2013) 1-20 . https://doi.org/10.1016/j.cis.2012.12.001

[5] M. Shah, D. Fawcett, S. Sharma, S. K. Tripathy, G. E. J. Poinern, Green synthesis of metallic nanoparticles via biological entities, Materials, 8 (2015) 7278–7308.   https://doi.org/10.3390/ma8115377

[6] Y.-A. Li, Y.-J. Chen, N.-H. Tai, Fast Process to decorate silver nanoparticles on carbon nanomaterials for preparing high-performance flexible transparent conductive films, Langmuir, (2013) 8433–8439. https://doi.org/10.1021/la401662d

[7] M. Ayán-Varela, M. J. Fernández-Merino, J. I. Paredes, S. Villar-Rodil, C. Fernández-Sánchez, L. Guardia, A. Martínez-Alonso, J. M. D. Tascón, Highly efficient silver-assisted reduction of graphene oxide dispersions at room temperature: Mechanism, and catalytic and electrochemical performance of the resulting hybrids, J. Mater. Chem. A, 2 (2014) 7295–7305.

[8] S. Navalon, A. Dhakshinamoorthy, M. Alvaro, H. Garcia, Metal nanoparticles supported on two-dimensional graphenes as heterogeneous catalysts, Coordin. Chem. Rev., 312 (2016) 99–148. https://doi.org/10.1016/j.ccr.2015.12.005

[9] J. Li, D. Kuang, Y. Feng, F. Zhang, Z. Xu, M. Liu, D. Wang, Green synthesis of silver nanoparticles–graphene oxidenanocomposite and its application in electrochemical sensing oftryptophan, Biosens. Bioelectron., 42 (2013) 198–206. https://doi.org/10.1016/j.bios.2012.10.029

[10] N. M. S. Hidayah, W.-W. Liu, C.-W. Lai, Comparison on graphite, graphene oxide and Reduce graphene oxide: synthesis and characterization, 1892 (2017). https://doi.org/10.1063/1.5005764

[11] M. T. H. Aunkor, I. M. Mahbubul, R. Saidurb , H. S. C. Metselaar, The green reduction of graphene oxide, RSC Adv., 6 (2016) 27807–27828. https://doi.org/10.1039/C6RA03189G

[12] S. Thakur, N. karak, Green reduction of graphene oxide by aqueous phytoextracts, Carbon, 50 (2012) 5331-5339. https://doi.org/10.1016/j.carbon.2012.07.023

[13] F. W. Low, C. W. Lai, S. B. Abd hamid, Easy preparation of ultrathin reduce graphene oxide sheets at high stirring speed, Ceram. Int., 41 (2015) 5798- 5806 .https://doi.org/10.1016/j.ceramint.2015.01.008

[14] Z. Zhang , F. G. Xu, W. S. Yang, M. Y. Guo, X. D. Wang, B. L. Zhanga, A facile one-pot method to high-quality Ag–graphene composite Nano sheets for efficient surface-enhanced Raman scattering, Chem. Commu., 47 (2011) 6440–6442. https://doi.org/10.1039/C1CC11125F

[15] S. Gurunathan, J. W. Han, J. H. Park, E. Kim, Y. J. Choi, D. N. Kwon, J. H. Kim, Reduced graphene oxide-silver nanoparticle nanocomposite: A potential anticancer Nanotherapy, Int. J. Nanomed., 10 (2015) 6257–6276. https://doi.org/10.2147/IJN.S92449

[16] S. W. Chook, C. H. Chia, S. Zakaria, M. K. Ayob, K. L. Chee, N. M. Huang, H. M. Neoh, H. N. Lim, R. Jamal, R. M. F. R. A. Rahman, Antibacterial performance of Ag nanoparticles and AgGO Nano composites prepared via rapid microwave assisted synthesis method, Nanoscale Res. Lett., 7 (2012). https://doi.org/10.1186/1556-276X-7-541

[17] D. Chen, L. Li, L. Guo, An environment –friendly preparation of reduced graphene oxide sheets via amino acid , Nanotechnology, 22 (2011). https://doi.org/10.1088/0957-4484/22/32/325601

[18] N. Dies , A. Śliwak, S. Gryglewicz, Enhanced reduction of graphene oxide by high -pressure hydrothermal treatment, RSC Adv., 5 (2015) 81831- 81837. https://doi.org/10.1039/C5RA14461B

[19] M. S. Ahmed, H. S. Han , S. Jeon, One- step chemical reduction of graphene oxide with oligothiophene for improved electrocatalyatic oxygen reduction reduction reaction , Carbon , 61 (2013) 164- 172. https://doi.org/10.1016/j.carbon.2013.04.080

[20] T. Kuila, S. Bose, P. khanara, A. K. Mishra, Recent advanced in graphene – based biosensor, Biosens. Bioelectron. , 26 (2011) 4637 – 4648. https://doi.org/10.1016/j.bios.2011.05.039

[21] M. Darroudi, M. B. Ahmad, R. Zamiri, A. Zak, A. H. Abdullah , N. A. Ibrahim, Time-dependent effect in green synthesis of silver nanoparticles, Int. J. Nanomed., 6 (2011) 677–681. https://doi.org/10.2147/IJN.S17669

[22] M. Abdullahab, F. T. Mohammed Noori, A. H. Al-Khursana, Second-order nonlinear susceptibility in quantum dot structure under applied electric field, Superlattices and Microstruct., 82 (2015) 219-233 . https://doi.org/10.1016/j.spmi.2015.01.041

[23] S. Kumar, V. Singh, A. Tanwar, Structural, morphological, optical and photocatalytic properties of Ag-doped ZnO nanoparticles, J. Mater. Sci. Mater. Electron., 27 (2016) 2166–2173.

[24] F. T. M. Noori, A. Kadhim , N. D. Hamza, Optical and Structural Properties of ZnO:Au Nano composite Thin films, Int. J. Nanoelectron. Mater., 11 (2018) 347-356 .

[25] Y. Haldorai, B. K. Kim, Y. L. Jo , J. J. Shim, Ag@graphene oxide Nano composite as an efficient visible-light plasmonic photocatalyst for the degradation of organic pollutants: A facile green synthetic approach, Mater. Chem. Phys., 143 (2014) 1452–1461 . https://doi.org/10.1016/j.matchemphys.2013.11.065